= ATOMS, MOLECULES, OPTICS =

RABI OSCILLATIONS AT THREE-PHOTON LASER EXCITATION OF A SINGLE RUBIDIUM RYDBERG ATOM IN AN OPTICAL DIPOLE TRAP

© 2024 I. I. Beterov^{a,b,c,d*}, E. A. Yakshina^{a,b,d}, G. Suliman^{a,b}, P. I. Betleni^{a,b}, A. A. Prilutskaya^{a,b}, D. A. Skvortsova^{a,c}, T. R. Zagirov^{a,b}, D. B. Tretyakov^{a,b}, V. M. Entin^a, N. N. Bezuglov^{a,e}, and I. I. Ryabtsev^{a,b**}

^aRzhanov Institute of Semiconductor Physics, Siberian Branch of Russian Academy of Sciences, Novosibirsk, 630090 Russia

^bNovosibirsk State University, Novosibirsk, 630090 Russia ^cNovosibirsk State Technical University, Novosibirsk, 630073 Russia ^dInstitute of Laser Physics, Siberian Branch of the Russian Academy of Sciences, Novosibirsk, 630090 Russia ^eSaint Petersburg State University, Saint Petersburg, 199034 Russia

* e-mail: beterov@isp.nsc.ru

** e-mail: ryabtsev@isp.nsc.ru

Received April 10, 2024 Revised April 24, 2024 Accepted April 24, 2024

Abstract. In an experiment on three-photon laser excitation $5S_{1/2} \rightarrow 5P_{3/2} \rightarrow 6S_{1/2} \rightarrow 37P_{3/2}$ of a single ⁸⁷Rb, Rydberg atom in an optical dipole trap, we have observed for the first time three-photon Rabi oscillations between the ground and the Rydberg states. A single atom was detected optically by resonance fluorescence signal using a low-noise sCMOS video camera. The relative probability for the atom to remain in the trap after the action of three synchronized exciting laser pulses with durations varying from 100 ns to 2 μ s was measured. A distinctive feature of the experiment was the use of intense laser radiation with a wavelength of 1367 nm at the second excitation step, providing a single-photon Rabi frequency up to 2 GHz to control the effective detunings of intermediate levels of the three-photon transition due to the dynamic Stark effect. Rabi oscillations with frequencies from 1 to 5 MHz were registered depending on the intensity of laser pulses of the first and second excitation steps with coherence time 0.7–0.8 μ s. Ways to increase the coherence time and contrast of three-photon Rabi oscillations for applications in quantum information with Rydberg atoms are discussed.

The article is presented as part of the conference proceedings "Physics of Ultracold Atoms" (PUCA-2023), Novosibirsk, December 2023.

DOI: 10.31857/S004445102410e109

1. INTRODUCTION

In recent years, ultracold neutral atoms have become one of the most promising platforms for implementing quantum computing. In particular, high-fidelity (>99.5%) two-qubit quantum gates have been demonstrated during their parallel execution for 60 single Rb atoms [1], and the capture of more than 6000 single Cs atoms in an array of optical dipole traps has been achieved [2]. Quantum computing

with ultracold neutral atoms requires coherent laser excitation of atoms into Rydberg states with principal quantum number n >> 1 [3]. Since the orbital radius of a Rydberg electron grows as n^2 , the dipole moments of Rydberg atoms also grow as n^2 , and they interact with each other much stronger than atoms in the ground state. Due to the large interaction energies of Rydberg atoms, it becomes possible to obtain quantum entangled states of neutral atoms and perform two-qubit quantum operations [4–6].

Typically, in experiments on creating quantum processors with neutral atoms as qubits, single atoms of Rb and Cs are used [6]. For laser excitation of Rb atoms, two-photon schemes of laser excitation of Rydberg nS- and nD-states are widely used according to the excitation scheme $5S \rightarrow 5P \rightarrow nS$, nD with a wavelength of 780 nm at the first stage and 480 nm at the second stage [7, 8] or $5S \rightarrow 6P \rightarrow nS$, nD with a wavelength of 420 nm at the first stage and 1013 nm at the second stage [1]. In experiments with single Cs atoms, a twophoton excitation scheme $6S \rightarrow 7P \rightarrow nS, nD$ with wavelengths of 459 nm at the first stage and 1040 nm at the second stage is typically implemented [9]. Single-photon excitation of Rydberg atoms is possible using ultraviolet laser radiation (wavelength 297 nm for rubidium atoms [10]). In two-photon excitation with counter-propagating laser beams, the residual Doppler effect, which arises due to the finite temperature of atoms in optical traps and leads to loss of coherence, is partially suppressed [11]. Unlike two-photon and three-photon schemes, single-photon excitation does not allow even partial compensation of the Doppler effect.

Three-photon laser excitation of single Rydberg atoms has several advantages. First, it allows excitation of Rydberg *nP* states, for which original schemes of three-qubit Toffoli quantum gate have been proposed [12,13]. In general, unlike atoms in Rydberg *nS* and *nD* states, single Rydberg *nP* atoms of alkali metals and their interaction with each other have been practically unexplored experimentally.

Second, three-photon laser excitation allows almost complete suppression of the recoil effect and Doppler effect in a star-shaped geometry of three beams with their wave vectors summing to zero [14]. This is promising for increasing the accuracy of quantum gates.

Third, in two-photon laser excitation, due to the high decay rate of intermediate excited states, it is necessary to introduce large detunings from exact resonance with intermediate states (> 1 GHz). Our theoretical analysis showed that three-photon laser excitation with a high Rabi frequency at the second stage compared to Rabi frequencies at the first and third stages allows achieving coherent excitation regime even when all three stages are tuned to exact resonance with atomic transitions. The absence of population and spontaneous decay of intermediate

states is ensured by light shifts from strong radiation at the second stage.

In previous works [15–18], we experimentally investigated the spectra and dynamics of three-photon laser excitation $5S_{1/2} \rightarrow 5P_{3/2} \rightarrow 6S_{1/2} \rightarrow nP$ of cold Rydberg Rb atoms in an operating magneto-optical trap using continuous single-frequency lasers at each stage and detection of single Rydberg atoms by selective field ionization method [3].

In our recent work [19], three-photon laser excitation of a single atom 87 Rb in an optical dipole trap to a Rydberg state $37P_{3/2}$ was experimentally demonstrated using laser radiation with wavelengths of 780 nm, 1367 nm, and 743 nm according to the scheme $5S_{1/2} \rightarrow 5P_{3/2} \rightarrow 6S_{1/2} \rightarrow 37P_{3/2}$ Excitation to Rydberg states was detected using an optical method based on atom losses in the optical dipole trap. Spectra of pulsed three-photon laser excitation of a single Rydberg atom were recorded. The spectrum width was 2 MHz. The dependence of excitation probability on laser pulse duration was also measured; however, no signs of Rabi population oscillations between ground and Rydberg states were observed. Such oscillations are necessary for subsequent implementation of quantum operations with Rydberg atoms.

This article presents the results of our new experiment on three-photon laser excitation $5S_{1/2} \rightarrow 5P_{3/2} \rightarrow 6S_{1/2} \rightarrow 37P_{3/2}$ of a single Rydberg atom ⁸⁷Rb, trapped in an optical dipole trap. Due to the narrowing of laser linewidths at the second and third stages, it became possible for the first time to observe three-photon Rabi population oscillations with frequencies ranging from 1 to 5 MHz depending on the intensity of laser pulses at the first and second excitation stages. A distinctive feature of the experiment was the use of intense laser radiation with a wavelength of 1367 nm at the second excitation stage, providing single-photon Rabi frequency up to 2 GHz to control effective detunings of intermediate levels of the three-photon transition through the dynamic Stark effect. Ways to increase coherence time and contrast of threephoton Rabi oscillations for applications in quantum informatics with Rydberg atoms are also discussed.

2. EXPERIMENTAL SETUP

The experimental setup scheme, described in detail in our previous work [19] on three-photon laser excitation of a single Rydberg atom ⁸⁷Rb, is shown

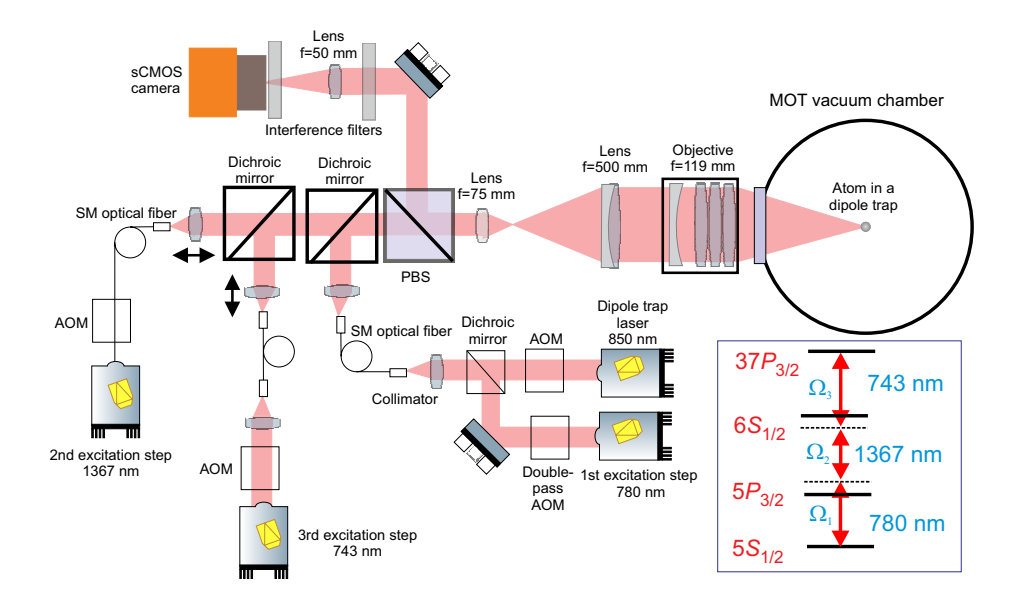


Fig. 1. Experimental setup for implementing coherent three-photon laser excitation into Rydberg state according to scheme $5S_{1/2} \rightarrow 5P_{3/2} \rightarrow 6S_{1/2} \rightarrow 37P_{3/2}$ (shown in the inset) of a single atom ⁸⁷Rb, trapped in an optical dipole trap

in Fig. 1. Main modifications in the present work include narrowing of laser linewidths, optimization of laser beam intensities, and upgrading optical schemes for laser radiation modulation.

2.1 Capturing atoms in an optical dipole trap

Atoms ⁸⁷Rb are cooled and trapped in a magnetooptical trap (MOT) in a vacuum chamber, where a cloud of cold atoms with a temperature of $80 - 100 \,\mu K$ is formed in the center. Then, to capture atoms from the MOT into an optical dipole trap, radiation from a laser system with a wavelength of 850 nm based on a DFB master laser Eaglevard EYP-DFB-0852 and a Toptica Boosta Pro semiconductor amplifier with an output power of 1.4 W is used. It is modulated using an acousto-optic modulator (AOM) and then coupled into the optical system via optical fiber. After exiting the optical fiber, the dipole trap laser radiation is collimated, reflected from a dichroic mirror, passes through a polarizing beam splitter, and then is focused into a cloud of cold rubidium atoms by an objective lens with a focal length of f = 119 mm and numerical aperture of NA = 0.172. A beam-expanding telescope consisting of two lenses with focal lengths of f = 75 mm and f = 500 mm is installed before the objective. The optical dipole trap radiation is focused into a spot with a diameter of $8-9 \,\mu m$ at intensity level e^{-2} .

2.2 Detection of trapped atoms

For the detection of trapped atoms 87 Rb resonance fluorescence induced by cooling lasers with a wavelength of 780 nm (not shown in Fig. 1) is used. Spontaneously emitted photons are collected by the same objective lens with a focal length of f=119 mm, pass through the telescope, partially reflect from the polarizing beam splitter, and then are focused by a f=50 mm lens onto a Tucsen Dhyana 400D digital sCMOS camera. Two interference filters that transmit radiation only at 780 nm wavelength are installed in front of the camera.

2.3 Laser excitation of Rydberg states

For the first stage of laser excitation, a Toptica DL Pro external-cavity diode laser and Toptica Boosta Pro semiconductor amplifier are used. Radiation from the same laser is used both for laser cooling and for laser excitation of atoms into Rydberg states. The first-stage laser frequency is locked to saturated absorption resonances in atoms 87 Rb (cross-resonance between hyperfine sublevels $|F=2\rangle$ and $|F'=3\rangle$ of state $5P_{3/2}$). AOMs are used for independent control of frequency detunings of the cooling radiation and first-stage laser excitation radiation. The first-stage laser radiation frequency was shifted using an AOM operating in double-pass configuration so that the radiation had a

blue detuning of $\delta_1 = +30$ MHz from resonance $|F = 2\rangle \rightarrow |F' = 3\rangle$, as shown in the inset of Fig. 1. The first-stage laser excitation radiation was combined with dipole trap radiation before the optical fiber using a dichroic mirror.

For the second stage of laser excitation, a Sacher Lasertechnik external-cavity diode laser at 1367 nm wavelength is used. The laser radiation frequency is locked using the Pound-Drever-Hall method to one of the transmission peaks of a highly stable Fabry-Perot interferometer manufactured by Stable Lasers using a Vescent Photonics D2-125PL locking system. As a result, the radiation has a red frequency detuning from resonance with transition $5P_{3/2}(F=3) \rightarrow 6S_{1/2}(F=2)$ of $\delta_2=-60$ MHz, as shown in the inset of Fig. 1. The linewidth estimation from the error signal is less than 25 kHz, and from the beat spectrum obtained by self-heterodyne method – less than 5 kHz. An AOM is used for amplitude modulation of the second-stage laser radiation.

The third stage uses a single-frequency titaniumsapphire laser with a ring resonator manufactured by Tekhnoscan, pumped by a solid-state Nd:YVO₄ laser Coherent Verdi G5. The laser frequency is stabilized to a transmission peak of a highly stable Fabry-Perot interferometer manufactured by Stable Laser Systems using an error signal generation system based on the Pound-Drever-Hall method and a Vescent Photonics D2-125 PID controller. To enable tuning to arbitrary Rydberg states, frequency locking utilizes spectral sidebands generated by mixing a radio frequency signal with arbitrarily set frequency in the range from 10 MHz to 200 MHz at the input of an electro-optical modulator in the frequency stabilization system. The radio frequency signal is synthesized using a Rigol DG4202 generator controlled via LAN interface. The estimated linewidth of the third stage laser based on the error signal does not exceed 2 kHz. An AOM is installed for amplitude modulation of the third stage laser. The radiation frequency is monitored by a WS-U precision wavelength meter manufactured by Angstrom.

The radiation from the second stage laser with a wavelength of 1367 nm and power up to 1 mW and the third stage laser with a wavelength of 743 nm and power of 10 - 50 mW is coupled into the optical system using separate optical fibers, as shown in Fig. 1. The laser beams are combined on a dichroic

mirror and coupled into the optical system coaxially with the optical dipole trap beam. Using precision translation stage-mounted lenses that collimate the radiation at the output of optical fibers, the divergence of the second and third stage laser beams is individually adjusted so that their focal spots with a diameter of no more than 10 μm at the intensity level e⁻² precisely coincide with the focal spot of the optical dipole trap. For this purpose, a DataRay BeamMap2 laser beam profiler is used. All exciting laser beams pass through a polarizing beam splitter and have horizontal polarization, similar to the optical dipole trap radiation.

2.4 Time diagram of the experiment

The time diagram of the experiment execution is shown in Fig. 2. A SpinCore PulseBluster programmable timer board is used to control the experimental setup. Atoms ⁸⁷Rb are initially loaded into the MOT for 0.1–5 s and simultaneously loaded into an optical dipole trap. The dipole trap laser radiation is modulated by rectangular pulses with a frequency of 1 MHz and duty cycle 60%, to avoid the influence of light shifts on atom detection in the absence of trap laser radiation. The Tucsen Dhyana 400D digital sCMOS video camera registers atoms with a sequence of frames with an exposure time of 175 ms until single atoms are loaded into the trap and the first resonance fluorescence signal from trapped atoms appears.

After detecting a single atom, the procedure of laser excitation of atoms to Rydberg states and optical detection of Rydberg excitation is initiated. The cooling lasers and MOT gradient magnetic field are turned off. Then the cooling laser beams, repump laser, and video camera are turned on for the first registration of fluorescence signals from the trapped atom to confirm that the atom is held in the optical dipole trap. After this, the cooling laser is turned off, while the repump laser remains on for 2 ms. This ensures optical pumping of the trapped atom into the state with $5S_{1/2}(F=2)$. After this, the radiation of the optical dipole trap is turned off to eliminate light shifts associated with this radiation, and all three stages of laser excitation of Rydberg atoms are turned on. After 0.1–5 us the excitation laser radiation is turned off, and the optical dipole trap radiation is turned on again. The time diagram of laser excitation pulses is discussed in detail in Section 4.

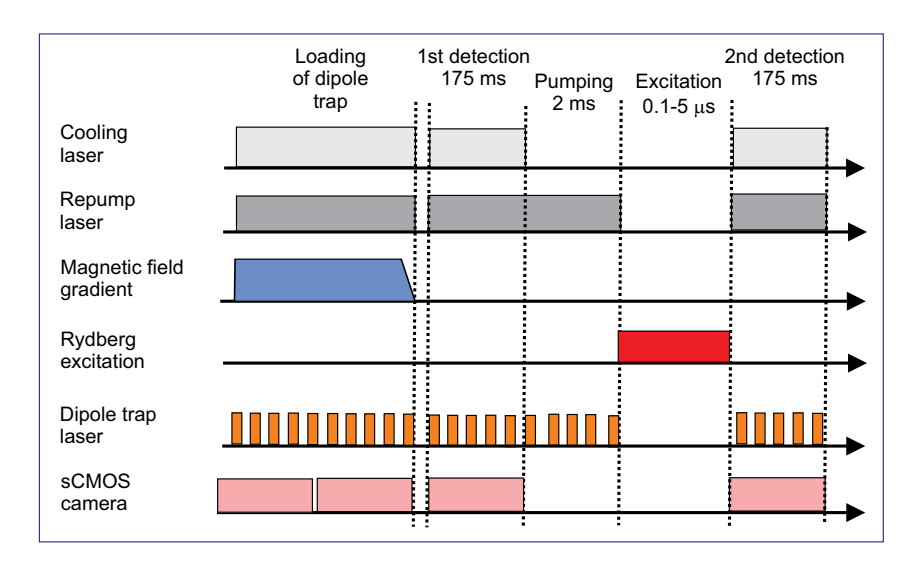


Fig. 2. Time diagram of the experiment on coherent three-photon laser excitation of a single atom ⁸⁷Rb to a Rydberg state

The intense radiation of the dipole trap laser pushes the atom ⁸⁷Rb out of the dipole trap if it is in the Rydberg state and recaptures it if it is in the ground state. hen the cooling laser beams, repump laser, and video camera are switched on again. An atom that was not excited to Rydberg states and remained in the optical dipole trap is registered again. In the experiment with single atoms, the probability of atom re-registration is measured depending on the laser radiation frequency.

3. THEORY OF THREE-PHOTON LASER EXCITATION OF RYDBERG STATE IN A SINGLE ATOM

In the theoretical description, we denote the ground state $5S_{1/2}(F=2)$ as state 1, the first intermediate state $5P_{3/2}^{1/2}(F=3)$ with a radiative lifetime of 27 ns as 2, the second intermediate state $6S_{1/2}(F=2)$ with a radiative lifetime of 50 ns as 3, and the Rydberg state $37P_{3/2}$ with a radiative lifetime of 43 us as 4 (the level and transition scheme is shown in the inset of Fig. 1). For each intermediate single-photon transition j = 1,2,3 we introduce the corresponding Rabi frequency $\Omega_i = d_i E_i / \hbar$ (here d_j — are the dipole moments of single-photon transitions, E_i — are the electric field amplitudes for linearly polarized light fields) and detuning δ_i . Scanning of the total detuning $\delta = \delta_1 + \delta_2 + \delta_3$ of the three-photon transition $1 \rightarrow 4$ can be performed by scanning the frequency of any laser. In our experiments, the detuning of the third-step laser δ_3 is scanned.

As we have shown in [14], in the absence of spontaneous relaxation of all levels and with sufficiently large detunings from intermediate resonances, $\Omega_1 << \left|\delta_1\right|, \Omega_2 << \left|\delta_2\right|$ the population of the Rydberg state can be calculated by solving the Schrödinger equation to find the probability amplitudes a_j of each level j=1-4 in the rotating wave approximation. As a result, we obtain the following dependence of population of the Rydberg state on the interaction time t for fully coherent three-photon laser excitation:

$$\begin{aligned} \left| a_4 \right|^2 &\approx \frac{\Omega^2}{\Omega^2 + (\delta + \Delta_1 + \Delta_4)^2} \times \\ &\times \frac{1}{2} \left[1 - \cos \left(t \sqrt{\Omega^2 + (\delta + \Delta_1 + \Delta_4)^2} \right) \right], \end{aligned} \tag{1}$$

where $\Omega = \Omega_1\Omega_2\Omega_3/(4\delta_1\delta_3)$ is the effective Rabi frequency for three-photon excitation, $\Delta_1 = \Omega_1^2/(4\delta_1)$ and $\Delta_4 = \Omega_3^2/(4\delta_3)$ are light shifts of states 1 and 4 respectively. Equation (1) shows that the condition for exact three-photon resonance is $\delta + \Delta_1 + \Delta_4 = 0$, while the population oscillates between the ground and Rydberg states at frequency Ω . Equation (1) also describes the excitation spectrum of the Rydberg state when scanning δ for a fixed interaction time t.

In formula (1), Rabi oscillations continue indefinitely. In a more realistic theoretical model that takes into account spontaneous relaxation of excited levels 2–4, Rabi oscillations decay with a decay constant $\gamma = 1/\tau$, determined by the inverse

lifetime of the Rydberg state τ , or even faster if the detunings of intermediate resonances are not large enough. In this case, the population of the Rydberg state reaches some steady-state value. Such a model was developed by us earlier in the four-level approximation based on optical Bloch equations for the density matrix [15]. Finding an exact analytical solution for the population ρ_{44} of the Rydberg state for arbitrary intermediate Rabi frequencies and detunings is not possible, therefore, in general, it is necessary to solve the problem numerically. However, at large detunings of laser radiation frequencies from intermediate resonances, our four-level system can be approximated by an effective two-level system with direct optical transition $1 \rightarrow 4$.

For a two-level system in work [15], we found the following approximate analytical solution in the case of strong $(\Omega >> \gamma)$ excitation:

$$\rho_{44} \approx \frac{\Omega^{2}}{2\Omega^{2} + \gamma^{2} + 4\delta^{2}} \times \left[1 - \exp\left(-\frac{2\Omega^{2} + \delta^{2}}{4\Omega^{2} + \delta^{2}}\gamma t\right)\right] + \left[1 - \exp\left(-\frac{2\Omega^{2} + \delta^{2}}{4\Omega^{2} + \delta^{2}}\gamma t\right)\right] - \exp\left(-\frac{6\Omega^{2} + \delta^{2}}{4\Omega^{2} + \delta^{2}}\gamma t\right) - \exp\left(-\frac{6\Omega^{2} + \delta^{2}}{4\Omega^{2} + \delta^{2}}\gamma t\right) - \exp\left(-\frac{6\Omega^{2} + \delta^{2}}{4\Omega^{2} + \delta^{2}}\gamma t\right)\right]. \tag{2}$$

Comparison of formula (2) with the simpler formula (1) for the model without relaxation shows that formula (1) is applicable at short interaction times ($\gamma t \ll 1$). At long interaction times ($\gamma t \gg 1$) Rabi oscillations decay and the population reaches a stationary value described by the Lorentzian excitation spectrum. Comparison of formula (2) with exact numerical calculation results showed that already at $\Omega > 3\gamma$ it has good accuracy. To apply formula (2) to the analytical description of coherent three-photon excitation spectrum, one should set $\Omega = \Omega_1 \Omega_2 \Omega_3 / (4\delta_1 \delta_3)$ — three-photon Rabi frequency, γ — inverse lifetime of the Rydberg state, and make the substitution $\delta \rightarrow \delta + \Delta_1 + \Delta_4$ to account for the light shift of the three-photon resonance.

At exact resonance (at $\delta = 0$) formula (2) gives the maximum amplitude of Rabi oscillations and has the following time dependence:

$$\rho_{44} \approx \frac{\Omega^2}{2\Omega^2 + \gamma^2} \Big[1 - e^{-\gamma t/2} \Big] +$$

$$+ \frac{1}{2} \Big[e^{-\gamma/2t} - e^{-3\gamma t/4} \cos(\Omega t) \Big].$$
 (3)

Since the condition $\Omega >> \gamma$, must be satisfied, formula (3) can be simplified to obtain the following dependence for approximating experimental Rabi oscillations:

$$\rho_{44} \approx \frac{1}{2} \left[1 - e^{-3\gamma t/4} \cos(\Omega t) \right]. \tag{4}$$

Furthermore, the developed theoretical model [15] allows phenomenological accounting for finite linewidths Γ_i of all three lasers in the phase diffusion model, where laser radiation contains random phase fluctuations but no amplitude fluctuations [20]. To take them into account, an imaginary part equal in modulus to Γ_i / 2 is added to each detuning δ_i in the density matrix equations for optical coherences to introduce additional decay in the coherence. Our numerical calculations according to this model showed good agreement between experiment and theory [15–18]. However, it should be noted that in such a model, the laser radiation spectrum has a Lorentzian shape, while lasers typically have a Gaussian profile with faster decay in the wings. Therefore, theoretical excitation spectra of Rydberg states in this model may have some discrepancies with experimental data in the wings of resonances.

4. METHODOLOGY FOR CONDUCTING EXPERIMENTS ON COHERENT THREE-PHOTON LASER EXCITATION OF A SINGLE ⁸⁷RB ATOM TO A RYDBERG STATE

The timing diagram of laser pulses for stages 1-3 in the experiment on coherent three-photon laser excitation of a single atom ⁸⁷Rb to a Rydberg state is shown in Fig. 3. The first-stage laser pulse (wavelength 780 nm) was formed using an AOM operating in a double-pass scheme with a focused beam and had the shortest edges (about 50 ns). The pulses of the second and third stage lasers (1367 nm and 743 nm) were formed using AOM in single-pass schemes without beam focusing and had edge durations of about 100 ns and 200 ns respectively. Therefore, to ensure the best time resolution and

contrast when recording Rabi oscillations, the following timing sequence logic was adopted, which is the main feature of specifically three-photon laser excitation of the Rydberg state.

The second-stage laser pulse was turned on first. Its intensity was chosen high enough to provide a single-photon Rabi frequency at the transition $5P_{3/2}(F=3) \rightarrow 6S_{1/2}(F=2)$ of about 2 GHz. Since this laser radiation had a red detuning of $\delta_2 = -60$ from the exact transition frequency, it created large light shifts of two levels (≈ 1 GHz), with level $5P_{3/2}(F=3)$ shifting down in energy and level $6S_{1/2}(F=2)$ shifting up. Thus, the intense second-stage radiation formed so-called "dressed" quasi-energy levels, which then provided large intermediate detunings for the first and third stage laser radiation from their resonances with atoms.

The third-stage laser was turned on second with a delay of 0.5 μ s after the second-stage laser was turned on. Initially, this radiation had a small detuning of $\delta_3 = +30$ MHz from the exact transition frequency $6S_{1/2}(F=2) \rightarrow 37P_{3/2}$, however, due to the light shift of state $6S_{1/2}(F=2)$ caused by the previously turned on second-stage laser radiation, the frequency detuning of the third-stage laser changed to $\delta_3 \sim -1$ GHz. Due to such large detunings, in the absence of first-stage laser radiation, the populations of all atomic levels remained unchanged in the field of the activated second and third stage laser radiation.

The first stage laser was turned on last with a 0.5 µs delay after the third stage laser activation. Initially, this radiation also had a small detuning $\delta_3 = +30$ MHz from the exact transition frequency $5S_{1/2}(F=2) \rightarrow 5P_{3/2}(F=3)$, however, due to the light shift of state $5P_{3/2}(F=3)$ caused by the previously activated second stage laser radiation, the frequency detuning of the third stage laser changed to $\delta_1 \sim +1$ GHz.

With the activation of the first stage laser, three-photon excitation of the Rydberg state began according to scheme $5S_{1/2} \rightarrow 5P_{3/2} \rightarrow 6S_{1/2} \rightarrow 37P_{3/2}$. Despite large light shifts of intermediate levels under the influence of intense second stage laser radiation, three-photon resonance occurred near the third stage laser detuning $\delta_3 = +30$ MHz from the exact transition frequency $6S_{1/2}(F=2) \rightarrow 37P_{3/2}$, as the condition for exact three-photon resonance $\delta = \delta_1 + \delta_2 + \delta_3 \approx 0$ was fulfilled precisely for this detuning. Overall, the values of small initial

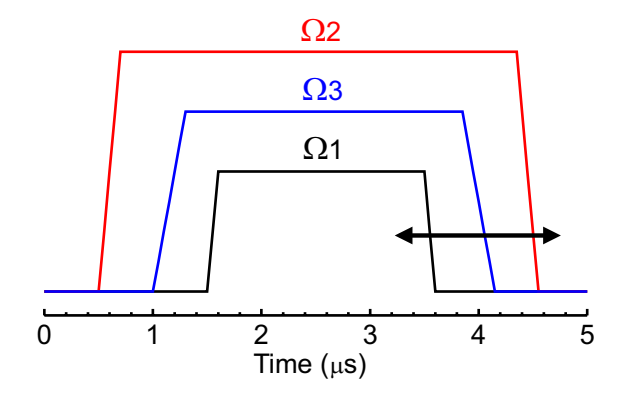


Fig. 3. Timing diagram of laser pulses for stages 1–3 in the experiment on coherent three-photon laser excitation of a single atom ⁸⁷Rb to a Rvdberg state

detunings from exact atomic resonances had practically no effect on the observation of Rabi oscillations, as the detunings of intermediate levels during three-photon excitation were determined by their enormous (~1 GHz) light shifts under the influence of intense second stage laser radiation. This is precisely the remarkable feature of three-photon excitation that we predicted during preliminary theoretical analysis and implemented in this experiment.

The duration of the three-photon excitation pulse was determined by the duration of the first stage laser pulse. Its duration could be set from 100 ns to 5 μ s, while at short times it was necessary to account for the effective duration considering the 50 ns edges, i.e., to recalculate based on the pulse area.

The switching off of the three laser pulses occurred in reverse sequence. The first stage pulse was switched off first, followed by the third stage pulse 0.5 µs later, and then the second stage pulse 1 µs after that. Due to the longer retention of the intense second stage pulse, larger detunings of intermediate single-photon transitions from the frequencies of stages 1 and 3 lasers were ensured. For stage 3, this helped avoid parasitic back-pumping of populations during single-photon de-excitation of the Rydberg state according to scheme $37P_{3/2} \rightarrow 6S_{1/2}(F=2)$ with subsequent rapid spontaneous decay of state $6S_{1/2}$ through the intermediate state 5P to the ground state $5S_{1/2}$. When varying the duration of the first stage pulse, the pulses of stages 2 and 3 were also varied synchronously to maintain the unchanged temporal sequence of pulse switching off.

One microsecond after switching off the second stage laser pulse, the dipole trap laser radiation was

switched on, followed by detection of a single 87 Rb atom presence through its resonance fluorescence signal. If the atom was in the Rydberg state, the trap laser radiation quickly (within a few microseconds) pushed it out of the trap, and no fluorescence signal was present. If the atom was in the ground state, it was recaptured in the trap, and the fluorescence signal was present. Thus, the population ρ_{11} of a single atom in the ground state $5S_{1/2}$ was measured after the completion of laser pulses for three-photon excitation. Since the intermediate levels of the three-photon transition are practically not populated due to their large detunings from resonances with all laser radiation, the experimentally measured population (excitation probability) of the Rydberg state can be accurately determined as $\rho_{44} \approx 1 - \rho_{11}$.

In the experimental recordings presented below, each point was averaged over 100 measurements. Since each measurement could be accompanied by atom loss during its excitation to the Rydberg state, it could take several seconds for recapturing a single atom, and the total time required for one recording was about half an hour. Therefore, slow drifts in frequency and power of laser radiation could affect the obtained results.

5. EXPERIMENTAL RESULTS AND COMPARISON WITH THEORY

In Fig. 4a the experimental recording (blue dots) of the three-photon laser excitation spectrum $5S_{1/2} \rightarrow 5P_{3/2} \rightarrow 6S_{1/2} \rightarrow 37P_{3/2}$ of the Rydberg state $37P_{3/2}$ in a single atom ⁸⁷Rb is presented

at an interaction time (first stage laser pulse duration) of 0.4 μs . The detuning δ_3 of the third stage laser frequency from the exact transition frequency $6S_{1/2}(F=2) \rightarrow 37P_{3/2}$ was scanned. A nearly Lorentzian contour with a full width at half maximum of 3 MHz was observed, and the resonance amplitude in the center reached $\rho_{44} \approx 1 - \rho_{11} \approx 0.7$.

Then the third stage laser frequency was tuned to the center of the three-photon resonance, and the dependence of ρ_{11} on the first stage laser pulse duration was measured. The obtained dependence (blue dots) is shown in Fig. 1 b. It confidently demonstrates the presence of Rabi oscillations. When approximating this dependence with analytical formula (4), it was determined that the Rabi oscillation frequency was $\Omega \ / \ (2\pi) \approx 1.35 \ \text{MHz},$ and their coherence time (decay at level 1 / e) was $\tau_{coher} \approx 0.8 \ \mu s$. The first oscillation with amplitude $\rho_{44} \approx 1 - \rho_{11} \approx 0.7$ occurs at a duration of 0.4 μs , which corresponds exactly to the spectrum in Fig. 4a.

Previously measured laser radiation spectral widths at each stage were $\Gamma_1\approx 100\,\text{kHz}, \Gamma_2\approx 5\,\text{kHz}, \Gamma_3\approx 2\,\text{kHz}.$ Thus, the total linewidth of the three lasers was $\Gamma\approx 107\,\text{kHz}.$ Therefore, the expected coherence time should have been $\tau_{coher}\approx 1\,/\,\Gamma\approx 9\,\mu\text{s},$ which is an order of magnitude longer than in the experiment. Also, the amplitude of the first oscillation should have been close to 0.95, which is noticeably higher than in the experiment. It was concluded that there is an additional parasitic broadening of about 1 MHz in the three-photon resonance, which is responsible for the significant

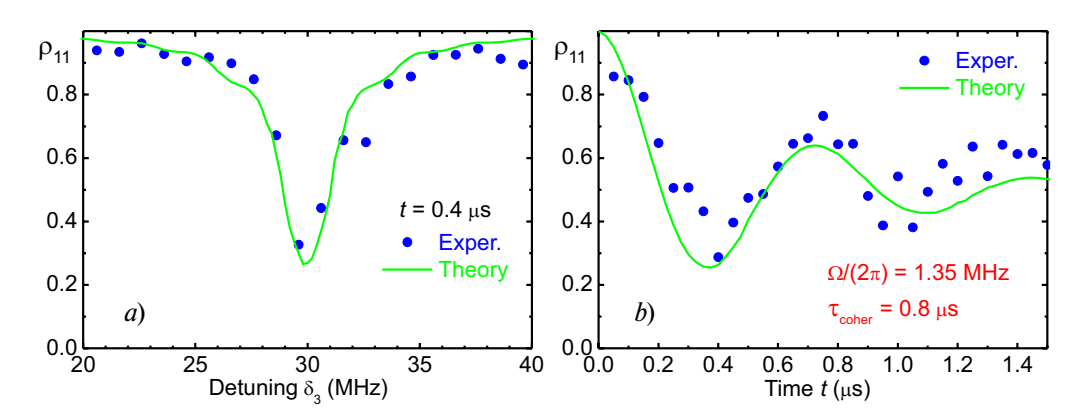


Fig. 4. a- Experimental recording (blue dots) of the three-photon laser excitation spectrum $5S_{1/2} \rightarrow 5P_{3/2} \rightarrow 6S_{1/2} \rightarrow 37P_{3/2}$ of the Rydberg state $37P_{3/2}$ at an interaction time (first stage laser pulse duration) of 0.4 μ s. The third stage laser frequency detuning δ_3 from the exact transition frequency $6S_{1/2}(F=2) \rightarrow 37P_{3/2}$ is scanned. b- Experimental recording (blue dots) of Rabi oscillations with frequency 1.35 MHz at the center of the three-photon resonance. Green solid curves are the results of numerical modeling in a four-level model with relaxation at single-photon Rabi frequencies Ω_1 / $(2\pi) \approx 80$ MHz, Ω_2 / $(2\pi) \approx 1740$ MHz, Ω_3 / $(2\pi) \approx 30$ MHz

decrease in coherence time and Rabi oscillation amplitude.

Typically, parasitic broadening of resonances in experiments with Rydberg atoms is caused by parasitic electric fields [17], as the polarizabilities of Rydberg states increase as n^7 with increasing principal quantum number n. However, in our experiment, a single atom 87 Rb was located in the center of the vacuum chamber and far from all surfaces (\sim 10 cm), where parasitic electric charges might be present Therefore, the influence of parasitic electric fields from the walls or windows of the vacuum chamber was practically eliminated.

The only source of parasitic broadening could be the incompletely compensated laboratory magnetic field in the center of the vacuum chamber. Although it is compensated along three axes by the available compensating Helmholtz coils during MOT adjustment, the accuracy of its compensation is 50-100 mG. Such a residual magnetic field leads to Zeeman splitting and broadening of each of the optical transitions between the used *S* and *P* levels by up to 250-500 kHz.

In Fig. 4, green solid lines show the results of numerical modeling with the introduction of parasitic Zeeman broadening of $\Gamma_Z \approx 300~\text{kHz}$ at each stage of laser excitation into the four-level model. Only with the introduction of such broadening was it possible to simultaneously achieve good agreement between experiment and theory for both the spectrum and Rabi oscillations.

The fitting parameters of the theoretical model were single-photon Rabi frequencies of $\Omega_1 \, / \, (2\pi) \approx 80 \quad M \, H \, z \, , \quad \Omega_2 \, / \, (2\pi) \approx 1740 \quad M \, H \, z \, , \label{eq:omega_1}$ $\Omega_{3}/(2\pi)\approx 30$ MHz, while the detunings and linewidths of the lasers were taken equal to the experimentally measured values. There was some uncertainty in measuring the intensities of laser pulses for single-photon Rabi frequencies, as the actual waist diameters of focused laser beams in the trapped atom region are known with finite precision. The laser powers for 1–3 stages were 150 µW, 180 µW and 3 mW respectively. The premeasured waist diameters of the second and third stage lasers were 10 µm, while the waist diameter of the first stage laser in the region where the atom is located was 200 µm. Based on this, estimates for single-photon Rabi frequencies in the theoretical model were obtained, taking into account known

(for transitions of stages 1 and 2) and calculated (for stage 3) matrix elements of dipole moments.

Based on the results of this experiment, it was concluded that parasitic Zeeman broadening limits the contrast and number of observable Rabi oscillations. To increase them to the theoretical limit, it is necessary to either better compensate for the residual magnetic field, or apply a sufficiently large external magnetic field and perform transitions between specific Zeeman sublevels of the ground and Rydberg states, or simply increase the laser radiation intensity and achieve a significant increase in Rabi frequency with the same coherence time. The first two options require additional research and will be implemented by us in the near future. In this article, we used the latter option.

It should be noted that to increase the three-photon Rabi frequency, the radiation intensity of either stage 1 or stage 3 should be increased. Increasing the intensity of stage 2, on the contrary, will lead to a decrease in the three-photon Rabi frequency due to increased light shifts of intermediate levels and detuning of laser radiation from single-photon resonances.

Therefore, in the next experiment, the laser radiation power at stage 1 was increased approximately by 10 times, which increased the single-photon Rabi frequency at stage 1 from 80 to 260 MHz. Figure 5 shows experimental recordings (blue dots) of three-photon laser excitation spectra $5S_{1/2} \rightarrow 5P_{3/2} \rightarrow 6S_{1/2} \rightarrow 37P_{3/2}$ of the Rydberg state $37P_{3/2}$ with approximately 10 times increased (compared to Fig. 4) power of stage 1 laser and interaction times 100 (a) and 150 (b) ns.

In Fig. 5a, one can see that at an interaction time of 100 ns, the resonance amplitude increased to $\rho_{44}\approx 1-\rho_{11}\approx 0.8$, and the width to 6.5 MHz. The latter is related to the increase in the Fourier width of the short laser pulse. When the duration was increased to 150 ns in Fig. 5b, the resonance amplitude decreased to 0.6, and the width to 5 MHz. Numerical simulation of these spectra revealed that for perfectly sharp laser pulse edges, Rabi oscillations described by formula (1) should have been observed on the resonance wings. However, the presence of edges comparable to the pulse duration itself led to the smoothing of these oscillations. For adequate description of this phenomenon, a trapezoidal time dependence of the stage 1 Rabi frequency was added to the theoretical model, as

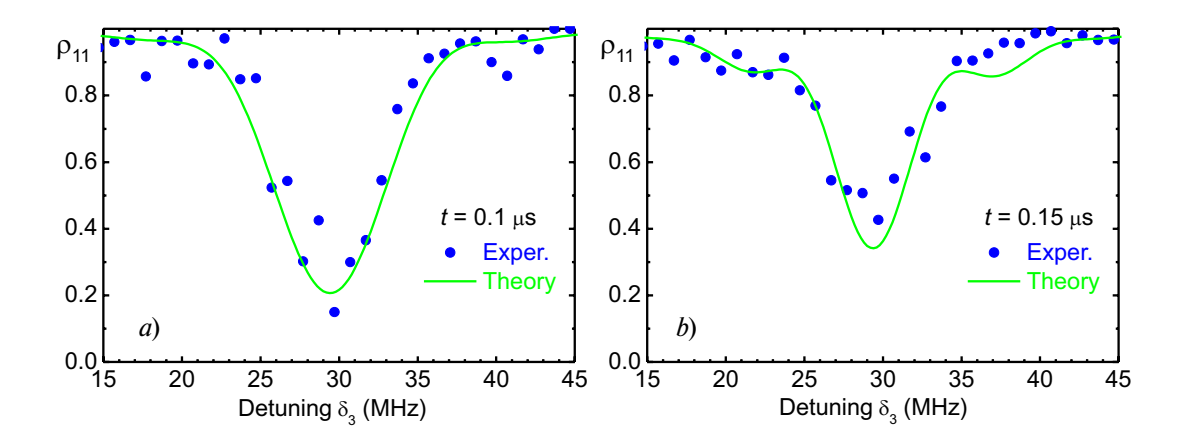


Fig. 5. Experimental recordings (blue dots) of three-photon laser excitation spectra of the $5S_{1/2} \rightarrow 5P_{3/2} \rightarrow 6S_{1/2} \rightarrow 37P_{3/2}$ Rydberg state $37P_{3/2}$ with approximately by 10 times increased (compared to Fig. 4) first stage laser radiation power and interaction times of 100 (a) and 150 (b) ns. The frequency detuning of the third stage laser is scanned δ_3 from the exact transition frequency $6S_{1/2}(F=2) \rightarrow 37P_{3/2}$. Green solid curves are the results of numerical modeling in a four-level relaxation model with single-photon Rabi frequencies of Ω_1 / $(2\pi) \approx 260$ MHz, Ω_2 / $(2\pi) \approx 1740$ MHz, Ω_3 / $(2\pi) \approx 30$ MHz. The model also took into account the 50 ns front duration for the laser pulse

shown in Fig. 3. Only this allowed achieving good agreement between experiment and theory (green solid curves) in Fig. 5, where in Fig. 5b both in experiment and theory, residual Rabi oscillations are visible on the wings.

Fig. 6a shows the experimental recording (blue dots) of Rabi oscillations during three-photon laser excitation $5S_{1/2} \rightarrow 5P_{3/2} \rightarrow 6S_{1/2} \rightarrow 37P_{3/2}$ of the Rydberg state $37P_{3/2}$ with approximately 10 times increased (compared to Fig. 4) radiation power of the first-stage laser. The experimental points are interpolated with spline function curves for clarity, as their number per oscillation is small due to the three-photon Rabi frequency increasing

to $\Omega / (2\pi) \approx 4.45$ MHz. The first oscillation with amplitude $\rho_{44} \approx 1 - \rho_{11} \approx 0.65$ occurs at a duration of 100 ns, which corresponds to the spectrum in Fig. 5a. The decrease in resonance amplitude compared to Fig. 5a may be related to insufficient temporal resolution in Fig. 6a, which is limited by the electronics used, having a minimum time scanning step of 50 ns.

The solid green curve in Fig. 6a is the result of numerical simulation in a four-level model with relaxation at single-photon Rabi frequencies $\Omega_1/(2\pi)\approx 260\,$ MHz, $\Omega_2/(2\pi)\approx 1740\,$ MHz, $\Omega_3/(2\pi)\approx 30\,$ MHz taking into account parasitic Zeeman broadening of the three-photon resonance.

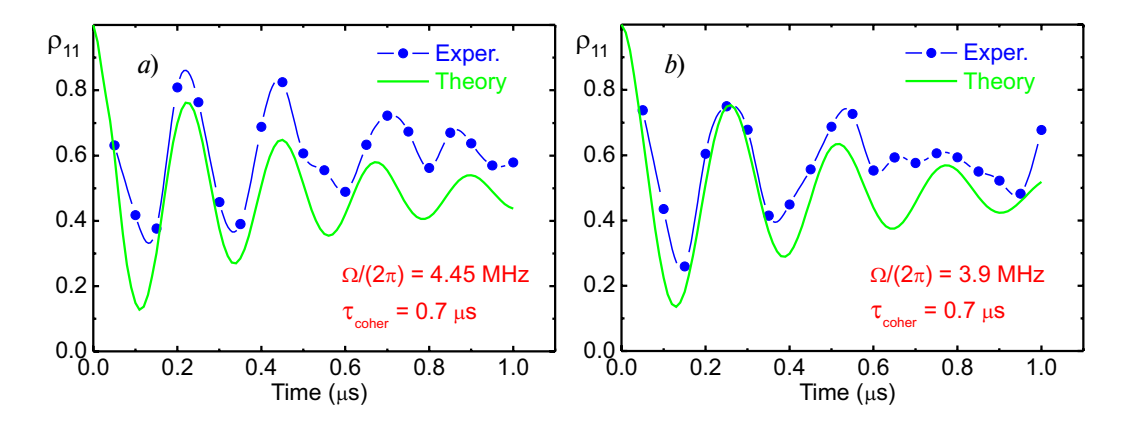


Fig. 6. a — Experimental recording (blue dots) of Rabi oscillations in three-photon laser excitation $5S_{1/2} \rightarrow 5P_{3/2} \rightarrow 6S_{1/2} \rightarrow 37P_{3/2}$ of the Rydberg state $37P_{3/2}$ with approximately 10 times increased (compared to Fig. 4) radiation power of stage 1 laser. Green solid curves are results of numerical simulation in a four-level model with relaxation at single-photon Rabi frequencies Ω_1 / $(2\pi) \approx 260$ MHz, Ω_2 / $(2\pi) \approx 1740$ MHz, Ω_3 / $(2\pi) \approx 30$ MHz. b — The same with stage 2 laser power increased by 1.3 times, which increased the stage 2 Rabi frequency to Ω_2 / $(2\pi) \approx 2$ GHz

It can be noted that the theoretical curve well reproduces the amplitude and frequency of the observed Rabi oscillations but inaccurately describes the stationary level against which the damped Rabi oscillations occur. In the experiment, it amounts to $\rho_{44}\approx 1-\rho_{11}\approx 0.4,$ while numerical calculation and analytical formula (4) predict it should be 0.5. We explain this phenomenon by two factors.

First, the detection of the Rydberg atom occurs with a delay of several microseconds relative to the end of the first-stage laser pulse. During this time, the population of the Rydberg state $37P_{3/2}$, which has an effective lifetime of 43 μ s at room temperature, partially decays to the ground state. In the future, we plan to conduct experiments with longer-lived higher states where this effect will be suppressed.

Secondly, during the laser pulse, not only the Rydberg state is populated, but also intermediate excited states $5P_{3/2}$ and $6S_{1/2}$ of the three-photon transition. In theoretical calculations, their total population is about 3%. After the laser pulse ends, these states rapidly decay to the ground state, which provides an additional contribution to the decrease in the steady-state level of decaying Rabi oscillations. To reduce this phenomenon, further increase in detuning of intermediate states from resonances with laser radiation is necessary. This can be achieved by increasing the intensity of the second-stage laser and corresponding increase in light shifts induced by it. However, this will decrease the three-photon Rabi frequency.

To verify the latter statement, we increased the power of the second-stage laser by 1.3 times, which increased the single-photon Rabi frequency of the second stage to $\Omega_2 / (2\pi) \approx 2$ GHz. The corresponding experimental recording is shown in Fig. 6b. It can be seen that this indeed led to a decrease in the three-photon Rabi frequency to $\Omega / (2\pi) \approx 3.9$ MHz. The observed change is also confirmed by theoretical calculation (green solid curve). Thus, by varying the power of the second stage, it is possible to control the parameters of three-photon laser excitation of Rydberg states within wide limits. This significantly distinguishes three-photon excitation from commonly used twophoton schemes, providing additional opportunities to increase the contrast of Rabi oscillations and, ultimately, increase the fidelity of quantum operations with Rydberg atoms.

6. CONCLUSIONS

This article presents the results of our new experiment on three-photon laser excitation $5S_{1/2} \rightarrow 5P_{3/2} \rightarrow 6S_{1/2} \rightarrow 37P_{3/2}$ of a single Rydberg atom ⁸⁷Rb, trapped in an optical dipole trap. Due to the narrowing of the laser linewidth at the second and third excitation stages, three-photon Rabi population oscillations with frequencies from 1 to 5 MHz were observed for the first time, depending on the intensity of laser pulses at the first and second excitation stages, with coherence time of 0.7–0.8 µs. A distinctive feature of the experiment was the use of intense laser radiation with a wavelength of 1367 nm at the second excitation stage, providing singlephoton Rabi frequency up to 2 GHz to control the effective detunings of intermediate levels of the three-photon transition due to the dynamic Stark effect.

The experiments revealed parasitic Zeeman broadening of the three-photon resonance due to insufficiently compensated laboratory magnetic field in the single atom region. This led to decreased contrast and coherence time of Rabi oscillations. To eliminate this effect, it is planned to implement optical pumping of the single atom to a specific Zeeman sublevel of the ground state and add a uniform magnetic field to create Zeeman level splitting and excite three-photon transitions between specified Zeeman sublevels of the ground and Rydberg states.

It is also necessary to investigate the influence of the residual Doppler effect on the contrast and coherence time of Rabi oscillations of a single Rydberg atom ⁸⁷Rb, trapped in an optical dipole trap. Preliminary calculations showed that even at the current atom temperature, estimated as $50 - 100 \,\mu\text{K}$, the Doppler effect can be significantly suppressed when using counter-propagating laser beams for the 1st and 3rd excitation stages, unlike the co-propagating beams in the present experiment. It should be noted that in a recent experiment on three-photon excitation of Rydberg states in an optical cell with thermal Cs atoms, using such laser beam configuration allowed almost complete suppression of the Doppler effect and obtaining an extremely narrow electromagnetically induced transparency resonance with a width of 190 kHz [21].

All the above measures should significantly improve the contrast and coherence time of

three-photon Rabi oscillations and, ultimately, increase the fidelity of quantum operations with Rydberg atoms compared to the fidelities achieved with two-photon laser excitation of Rydberg atoms.

FUNDING

This work was supported by the Russian Science Foundation (project 23-1200067, https://rscf.ru/project/23-12-00067/).

REFERENCES

- **1.** S. J. Evered, D. Bluvstein, M. Kalinowski, et al., Nature **622**, 268 (2023).
- 2. H. J. Manetsch, G. Nomura, E. Bataille, K. Leung, X. Lv, and M. Endres, arXiv: 2403.12021 (https://arxiv.org/abs/2403.12021).
- 3. T. F. Gallagher, *Rydberg Atoms*, Cambridge University Press, Cambridge (1994).
- 4. D. Jaksch, J. I. Cirac, P. Zoller, S. L. Rolston, R. Cote, M. D. Lukin, Phys. Rev. Lett. 85, 2208 (2000).
- 5. M. Saffman, J. Phys. B 49, 202001 (2016).
- L. Henriet, L. Beguin, A. Signoles, T. Lahaye, A. Browaeys, G.-O. Reymond, and C. Jurczak, Quantum 4, 327 (2020).
- 7. T. Cubel, B. K. Teo, V. S. Malinovsky, J. R. Guest, A. Reinhard, B. Knuffman, P. R. Berman, and G. Raithel, Phys. Rev. A 72, 023405 (2005).
- **8**. M. Reetz-Lamour, J. Deiglmayr, T. Amthor, and M. Weidemuller, New J. Phys. **10**, 045026 (2008).
- T. M. Graham, Y. Song, J. Scott et al., Nature 604, 457 (2022).
- **10**. P. Thoumany, T. Hansch, G. Stania, L. Urbonas, and Th. Becker, Opt. Lett. **34**, 1621 (2009).
- V. A. Sautenkov, S. A. Saakyan, A. A. Bobrov, E. V. ilshanskaya, B. B. Zelener, and B. V. Zelener, J. Opt. Soc. Am. B 35, 1546 (2018).

- 12. P. Cheinet, K.-L. Pham, P. Pillet, I. I. Beterov, I. N. Ashkarin, D. B. Tretyakov, E. A. Yakshina, V. M. Entin, I. I. Ryabtsev, Quantum Electronics 50, 213 (2020).
- I. N. Ashkarin, I. I. Beterov, E. A. Yakshina, D. B. Tretyakov, V. M. Entin, I. I. Ryabtsev, P. Cheinet, K.-L. Pham, S. Lepoutre, and P.Pillet, Phys. Rev. A 106, 032601 (2022).
- **14**. I. I. Ryabtsev, I. I. Beterov, D. B. Tretyakov, V. M. Entin, E. A. Yakshina, Phys. Rev. A **84**, 053409 (2011).
- 15. V. M. Entin, E. A. Yakshina, D. B. Tretyakov, I. I. Beterov, I. I. Ryabtsev, JETP 143, 831 (2013) [V. M. Entin, E. A. Yakshina, D. B. Tretyakov, I. I. Beterov, and I. I. Ryabtsev, JETP 116, 721 (2013)].
- 16. E. A. Yakshina, D. B. Tretyakov, V. M. Entin, I. I. Beterov, I. I. Ryabtsev, QE 48, 886 (2018) [E. A. Yakshina, D. B. Tretyakov, V. M. Entin, I. I. Beterov, and I. I. Ryabtsev, Quantum Electronics 48, 886 (2018)].
- 17. E. A. Yakshina, D. B. Tretyakov, V. M. Entin, I. I. Beterov, I. I. Ryabtsev, JETP 157, 206 (2020) [E. A. Yakshina, D. B. Tretyakov, V. M. Entin, I. I. Beterov, I. I. Ryabtsev, JETP 130, 170 (2020)].
- 18. D. B. Tretyakov, V. M. Entin, E. A. Yakshina, I. I. Beterov, I. I. Ryabtsev, QE 52, 513 (2022) [D. B. Tretyakov, V. M. Entin, E. A. Yakshina, I. I. Beterov, and I. I. Ryabtsev, Quantum Electronics 52, 513 (2022)].
- I. I. Beterov, E. A. Yakshina, D. B. Tretyakov, N. V. Alyanova, D. A. Skvortsova, G. Suliman, T. R. Zagirov, V. M. Entin, I. I. Ryabtsev, JETP 164, 282 (2023) [I. I. Beterov, E. A. Yakshina, D. B. Tretyakov, N. V. Al'yanova, D. A. Skvortsova, G. Suliman, T. R. Zagirov, V. M. Entin, and I. I. Ryabtsev, JETP 137, 246 (2023)].
- **20**. G. S. Agarwal, Phys. Rev. Lett. **37**, 1383 (1976).
- **21**. S. M. Bohaichuk, F. Ripka, V. Venu, F. Christaller, C. Liu, M. Schmidt, H.Kobler, and J.P.Shaffer, arXiv: 2304.07409 (https://arxiv.org/abs/2304.07409).